Report 3

Thank you very much for the positive appraisal and the useful suggestions.

Main points 1. While we understand that the cluster size Nc of the calculations is limited due to computational constraints, we were wondering whether there is a principle threshold of Nc where the linear-in-T behavior becomes apparent. Did the authors also try to employ smaller clusters (e.g., $N_c = 3$? If yes, did the linear-in-T behavior persist for both regimes?

2. Connected to the first point: as far as we understand, the linear-in-T behavior of the resistivity emerging from (quantum) critical properties of the Mott metal-insulator transition can be found in single-site ($N_c = 1$) dynamical mean-field theory, see Ref. 17 of the manuscript. Does this mean, in turn, that only for regime (ii) [i.e., the interaction-driven mechanism] an actual cluster calculation $N_c = 1$ is necessary?

Calculations at $p = 25\%$ in clusters of size $N_c = 1$, $N_c = 2$ and $N_c = 4$ of the scattering rate as a function of temperature were added in Appendix B Figure 10. We did not employ a three site cluster because of apprehensions we have regarding the use of clusters with an odd number of sites. We found that single-site clusters did not allow to find T-linear scattering rate at low T. However, cluster with two or more sites did allow a T-linear regime. We added the following:

> At $p = 0.25$, Fig. 10 shows that in the single-site cluster, the scattering rate becomes quadratic at low temperature. However, the T-linear regime is retrieved at low temperature for $N_c \geq 2$ clusters. This means that short-range interactions, such as superexchange, are important in order to find the interaction-driven T-linear scattering rate regime.

We also added the following to the main text in the second to last paragraph of subsection A of the discussion.

> It is well known that there is a critical point associated to the Mott transition at half-filling in single site DMFT [85, 86]. In the bad-metal regime at high temperature, a linear in T scattering rate is also found [16, 17, 87]. It is also known that the Mott critical point has an influence away from half-filling [15]. To verify if single site DMFT at finite doping also has an interaction-driven T-linear scattering regime at large doping, calculations as a function of temperature at $p = 0.25$ for cluster sizes $N_c = 1$, $N_c = 2$ and $N_c = 4$ were performed, and are displayed in Fig. 10 of Appendix A. They show that while single site DMFT calculations lead to T^2 scattering rate at low temperature, clusters with $N_c \geq 2$ lead to T-linear behaviour at low temperature. This strongly suggests that superexchange is crucial for the T-linear behaviour of the scattering rate in this regime.

3. Can the authors comment (for one representative data point) on the spin and charge correlation lengths in the two T-linear regimes or is this computationally out of reach?

Our DCA program does not allow us to find the charge and spin correlation lengths. However, DMRG studies in the triangular Hubbard model seem to indicate that the correlation length are of the order of the lattice spacing (1 in that research) [1]: the triangular lattice geometrically forbids long-range magnetic correlations until very low temperature, in particular for the range of interactions strengths of interest to us $8.5 \leq U/t \leq 10.54$ [1–11].

4. As sort of general orientation it would be interesting to see the Mott transition (including the coexistence regime) mapped out for the doped system and plotted within Fig. 2. Do the authors think that this is numerically feasible?

The Mott transition was added to the phase diagram of Fig. 2 on Fig. 12 of the appendix. We added the following to Appendix C:

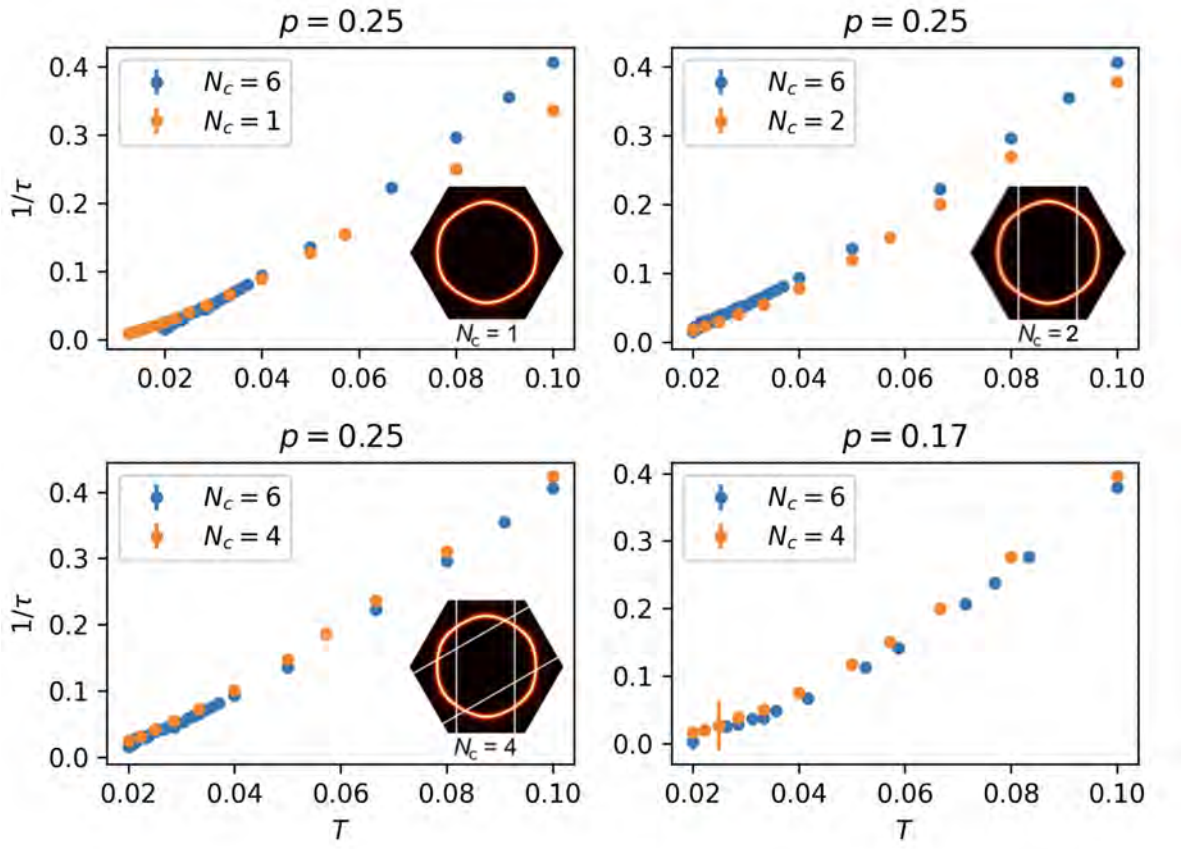

FIG. 1. Local scattering rate as a function of temperature for different clusters, at $p = 0.25$ and $p = 0.17$ for $U = 8.5$. One needs at least $N_c = 2$ to find a linear regime.

> In order to strengthen the link between the finite-doping continuation of the Mott transition, the Sordi transition [38], and the low-doping T-linear regime, the doping p was computed as a function of chemical potential at fixed temperature and $U = 8.4$. Fig. 12 presents an improved phase diagram at $U = 8.4$ and low dopings, where the Sordi transition and the Widom line are added to the colorplot in Fig. 2a).

5. To demonstrate the existence of a pseudogap (as indicated in paragraph 2, left column, of page 5), it would be very instructive to show the spectral weight at the Fermi level [from, e.g., an extrapolation of $A(K, i\omega_{n\to 0})$] for different K-patches in this regime.

The spectral weight as a function of temperature for different dopings was added to this manuscript on Fig. 20 in Appendix F. We also added the following to the appendix :

> In order to demonstrate the existence of a pseudogap in the triangular lattice, the spectral weight $A(K_i, \omega = 0)$ as a function of temperature is computed for different dopings. This data is presented on Fig. 20. We observe that for $p = 0.04$, $p = 0.06$ and $p = 0.25$, the spectral weight increases as the temperature decreases. This means that a quasiparticle peak is found at these points, indicating that there is no pseudogap. Thus, the downturn of the scattering rate for temperature below the critical point at $p = 0.04$ is not directly caused by a pseudogap, but is instead a precursor. However, we see that when the doping is decreases to $p = 0.023$, we eventually see a decrease of the spectral weight at low temperature, which indicates that there is a pseudogap.

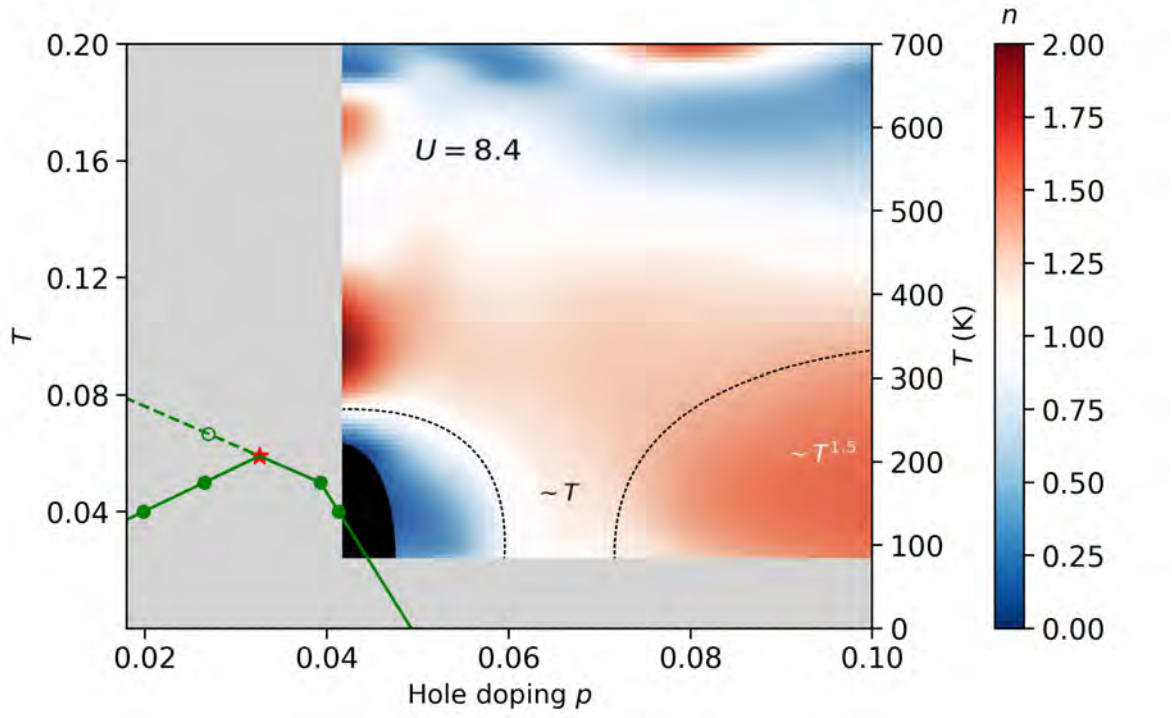

FIG. 2. Phase diagram of the triangular lattice Hubbard model at $U = 8.4$. In addition to the colorplot from Fig. 2a), the Sordi transition and the Widom line between the PG and cFL are also displayed, respectively, with a full line and a dotted line. There is no data of the scattering rate as a function of temperature in the dark region near $p = 0.04$, as seen in Fig. 12.

6. In the interest of graphical clarity: did the authors consider log-log plots for the scattering rates, where one could read off also exponents possibly different from 1?
A log-log plot of the scattering rate for the interesting dopings (i.e. $p = 0.04$, $p = 0.06$, $p = 0.08$ and $p = 0.25$ was added in Fig. 17 of Appendix E. We also added the following text in that appendix:

> In order to highlight the different scattering-rate regimes on the triangular lattice, the results as a function of temperature are also displayed on a log-log scale on Fig. 17. In the Mott-driven T-linear regime at small dopings, the low-temperature scattering rate for the different patches changes drastically with doping, as shown on Fig. 18

7. Could the authors make a more explicit comment on the mapping to the electron doped side, if possible? From Fig. 4 the mapping seems to be non-trivial.

The following explanation of the electron-doped side in this research was added at the end of section II.A. We hope that this will improve the readability of the manuscript.

> The band parameters are the same for both hole and electron doping with respect to half-filling. Doping is controlled by the chemical potential. We focus mostly hole doping.

Minor points (and typos, etc.)
8. To avoid possible confusion with other studies, it would be helpful if the authors could show the (non-interacting) density of states for their model [e.g., as Fig. 1c)].

The non-interaction DOS for the triangular Hubbard model was added to figure 1. The following was also added to section II.A :

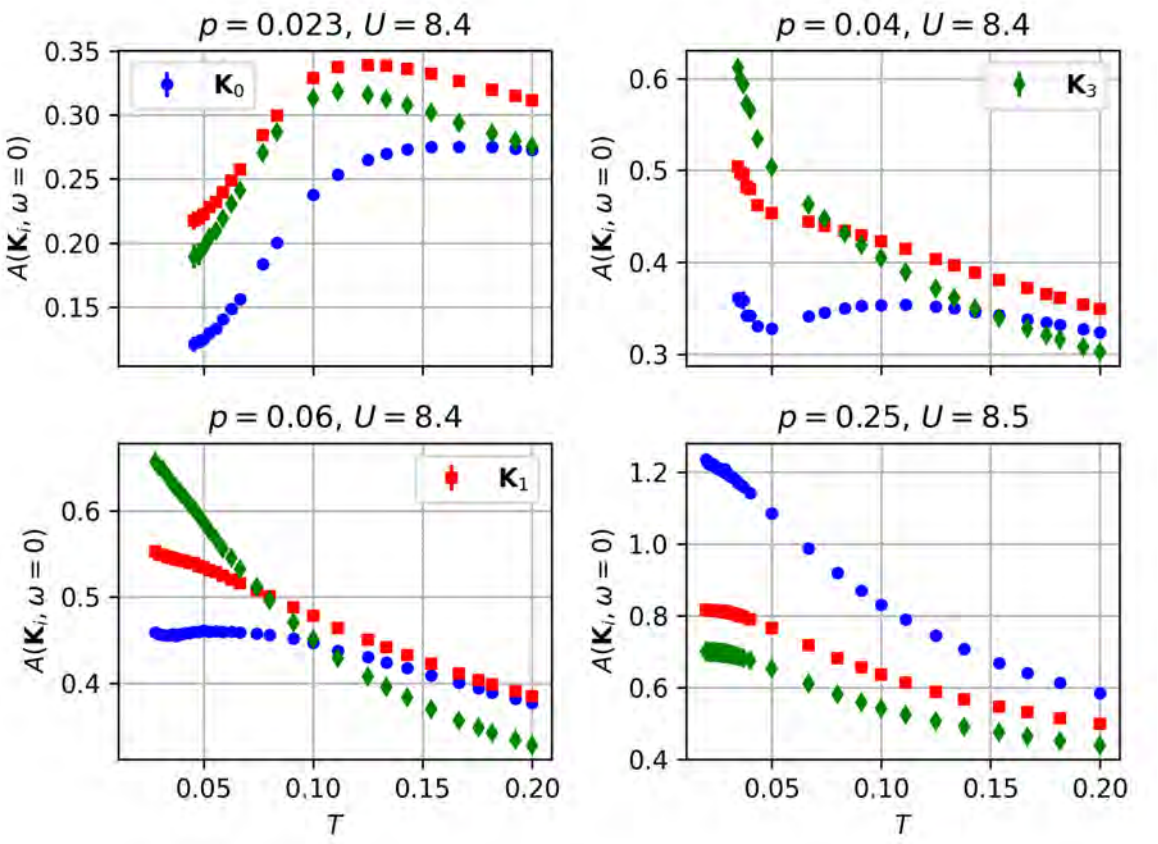

FIG. 3. Spectral weight as a function of temperature for the patches K_0, K_1 and K_3 at different dopings and U.

With these values of t and t', the non-interaction density of states is :

$$\epsilon_{\mathbf{k}} = -2\left[t\cos(k_x) + t\cos\left(\frac{k_x}{2} - \frac{\sqrt{3}k_y}{2}\right) + t'\cos\left(\frac{k_x}{2} + \frac{\sqrt{3}k_y}{2}\right)\right]$$

9. In order to judge the overall level of scattering and the degree of momentum differentiation, a plot of Γ for the respective momentum patches, at constant T and varying p would be helpful as amendment to Fig. 2.

A figure of the scattering rate as a function of doping for $U = 8.4$ and for dopings near the PG was added to the manuscript on Fig. 18 of appendix E. Moreover, we added to following to Appendix

In the Mott-driven T-linear regime at small dopings, the low-temperature scattering rate for the different patches changes drastically with doping, as shown on Fig. 18.

10. Fig. 2: are the temperature ranges shown in (a) and (b) the same? If yes, this should be stated in the caption.

Yes, the following was added to the caption of Fig. 2:

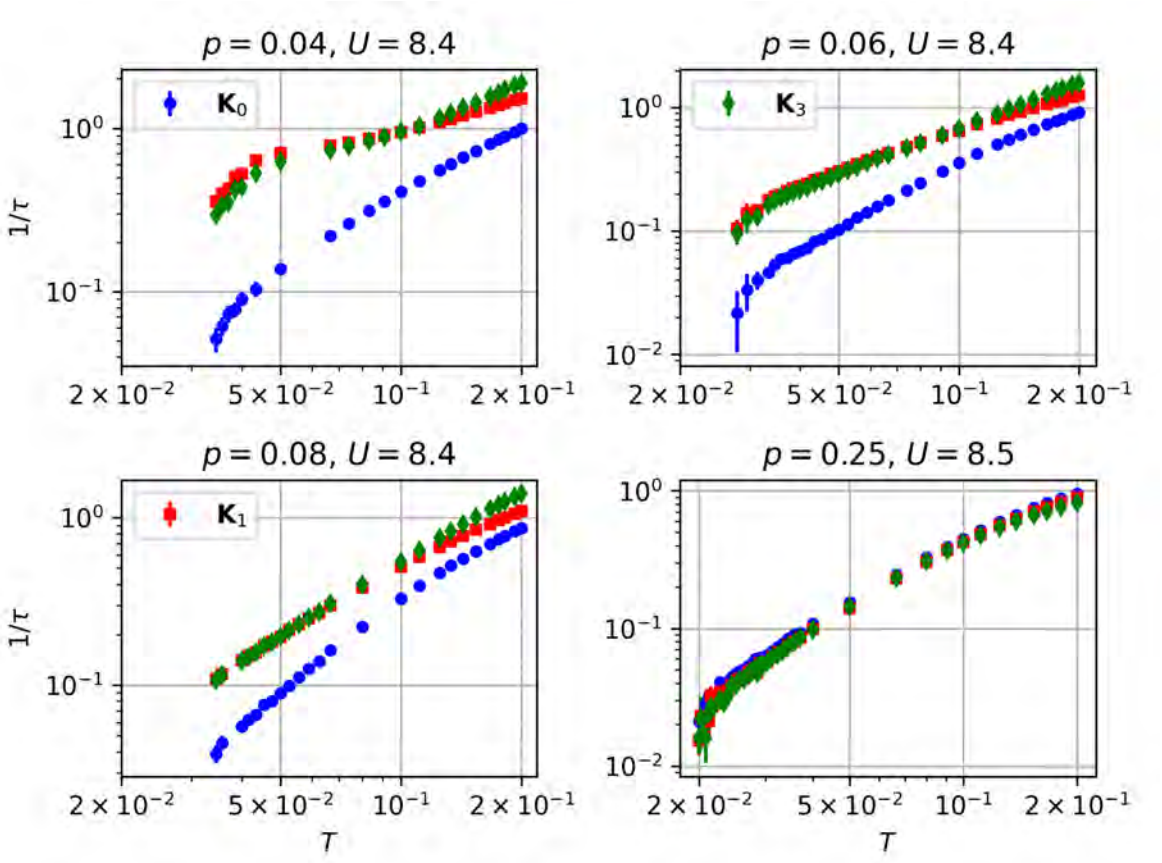

FIG. 4. Scattering rate as a function of temperature on a logarithmic scale for different regimes displaying T-linear scattering rate. The different colors refer to different patches.

a) and b) share the same vertical axis. This means that the temperature range for both figures is the same.

11. Fig. 3: We congratulate the authors to this very fine-grained high quality data. We have the following requests/questions:

(a) As the doping regime from p = 0.06 to p = 0.08 is particularly interesting, why are only the endpoints of this regime shown in Fig. 3? Can the authors confirm that the qualitative behaviour does not change in between these points?

As $p = 0.08$ has an exponent n a little bit larger than $p = 0.06$, we see a gradual increase of n between these two dopings. However, there is no big changes happening between these two dopings.

(b) In Fig. 4, the notion of the yellow and red stars are introduced as the critical interactions of the metal-to-insulator transition. We think it could be worthwhile to mark them in Fig. 3 at the respective fillings/temperatures.

The yellow star for which the DOS was computed in Fig.4 was obtained by fixing the temperature and U, and varying the chemical potential. We do not have data for the scattering rate as a function of temperature for the specific doping and temperature of the yellow star in Fig. 3.

12. Fig. 4:(a) Which K-patches do the spectral functions correspond to? Are these local ones? This

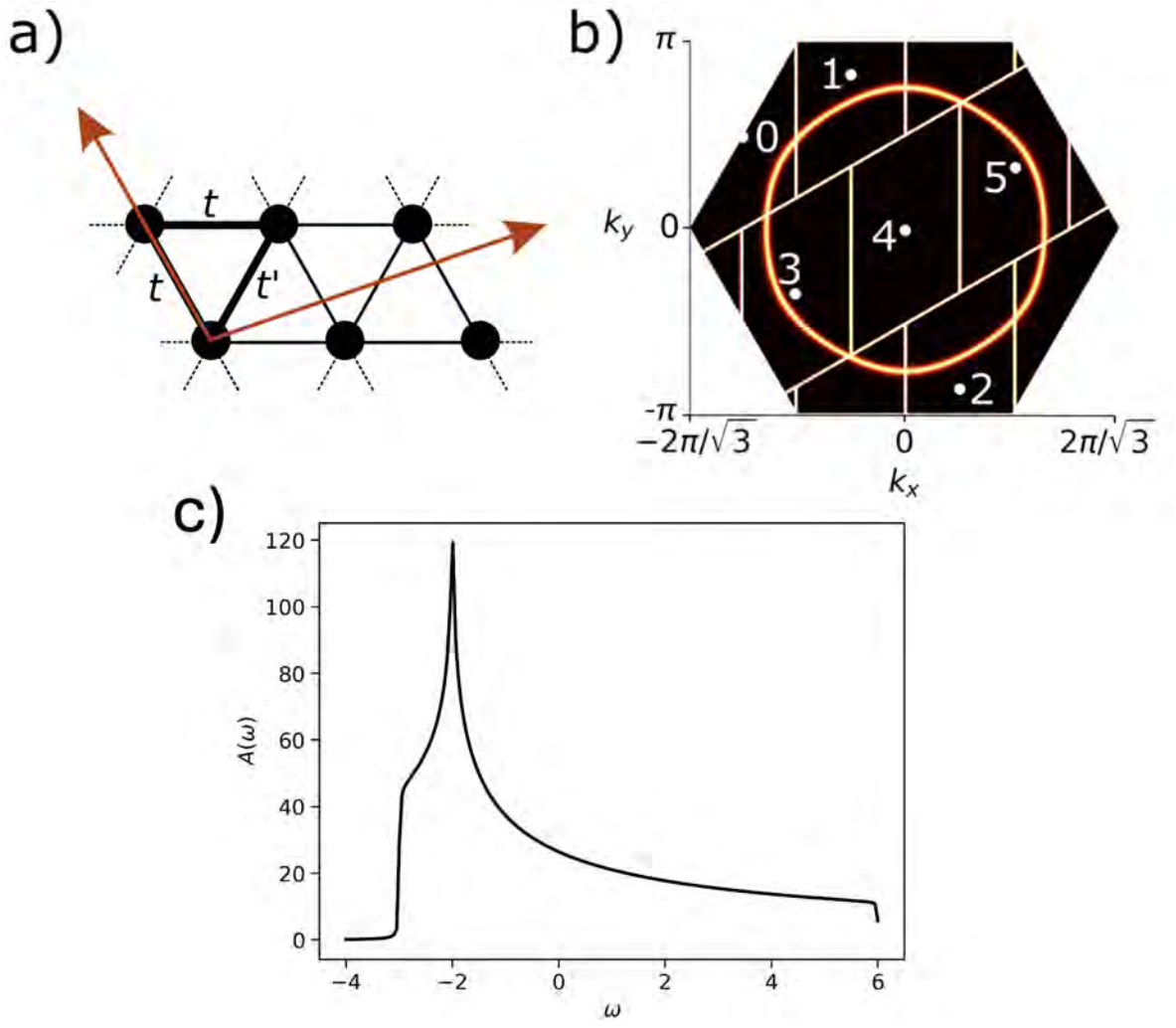

FIG. 5. a) Hopping terms on the triangular lattice b) Fermi surface for $U = 0$ and $n = 1$ at $T = 0.1$ on the triangular lattice. The different patches used in the Brillouin zone of the triangular lattice and on the proxy square lattice made of the reciprocal lattice-vectors are illustrated. The superlattice vectors in red illustrate the periodic boundary conditions. Although $t' = -t$ is satisfied in our work, this connectivity corresponds to a bipartite lattice when $t' = 0$. The illustrated Fermi surface is a hole Fermi surface. c) Local density of states for the non-interacting triangular-lattice.

should be stated in the caption and the spectral function y-axis labels should be adapted accordingly.

Sorry for the omission. The local spectral function is plotted in Fig. 4. This information was added to the caption of Fig. 4.

(b) The authors give the spectral function for the T-linear "Mott-driven" regime. What is the splitting of the Hubbard bands? Would it be worthwhile to give the spectral function for a representative point of the "interaction driven" T-linear point for comparison? Do you still find Hubbard bands, does the splitting persist?

The DOS for $T = 1/41$, $T = 1/30$ and $T = 1/20$ at $p = 25\%$ was added in Fig. 21 of Appendix F to show the spectral function of the interaction-driven region. We also added the following to Appendix

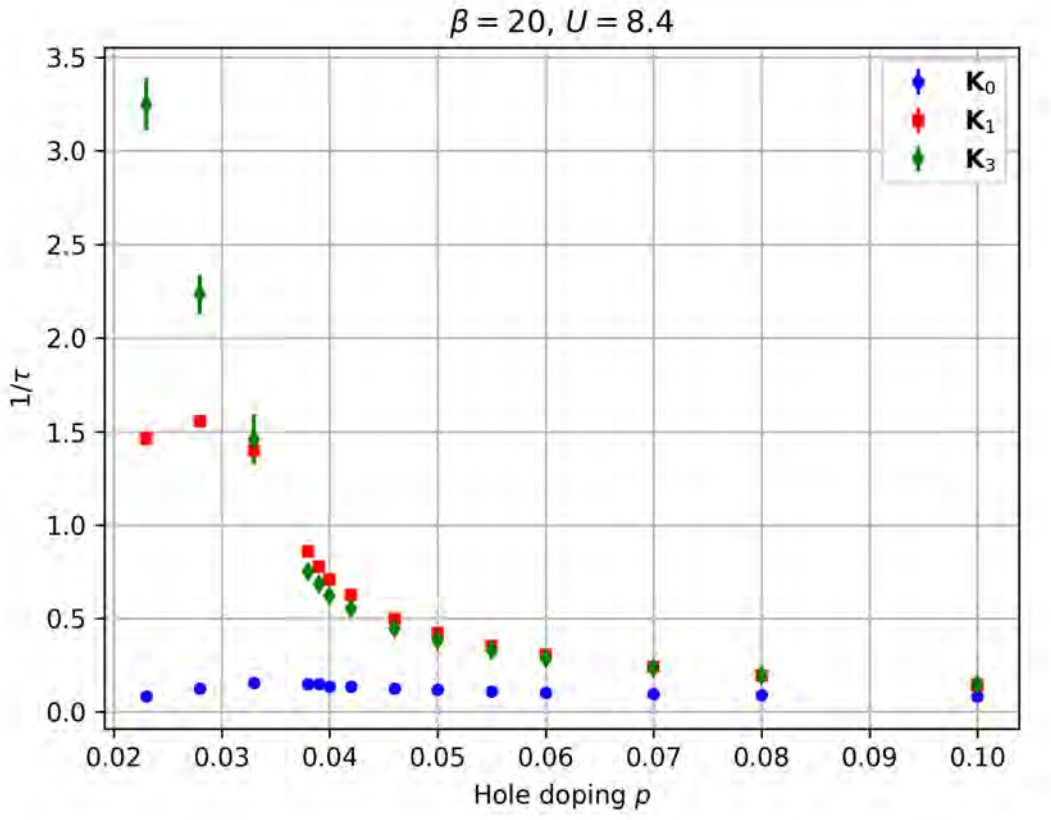

FIG. 6. Scattering rate as a function of hole doping at $U = 8.4$ and fixed temperature $T = 1/20$, for patches K_0, K_1 and K_3.

F :

> We also computed the density of state for different temperatures in the interaction-driven T-linear regime. This data is presented on Fig. 21. We find that, just like in the Mott-driven regime, the density of state presents a peak near $\omega = 0$.

(c) Further, we consider the colour coding confusing, especially in direct comparison with Fig. 3. Could the authors choose different colors and/or line styles for the fillings in the inset of Fig. 4 to discriminate from different patches in Fig. 3? If the spectral functions correspond to a certain K-patch, it would be worthwhile to use the same colour coding here as in Fig. 3.

The colors on Fig. 4 were changed in order to avoid confusion with the color corresponding to the different patches in Fig. 3.

13. Fig. 5: We could not find data for p = 0.5.

Thank you for pointing out this mistake. The data was for $p = 0.05$.

14. Appendix A: How does the cluster geometry for $N_c = 12$ look like?

The cluster geometry for $N_c = 12$ was added to the middle panel of Fig. 8 if Appendix A.

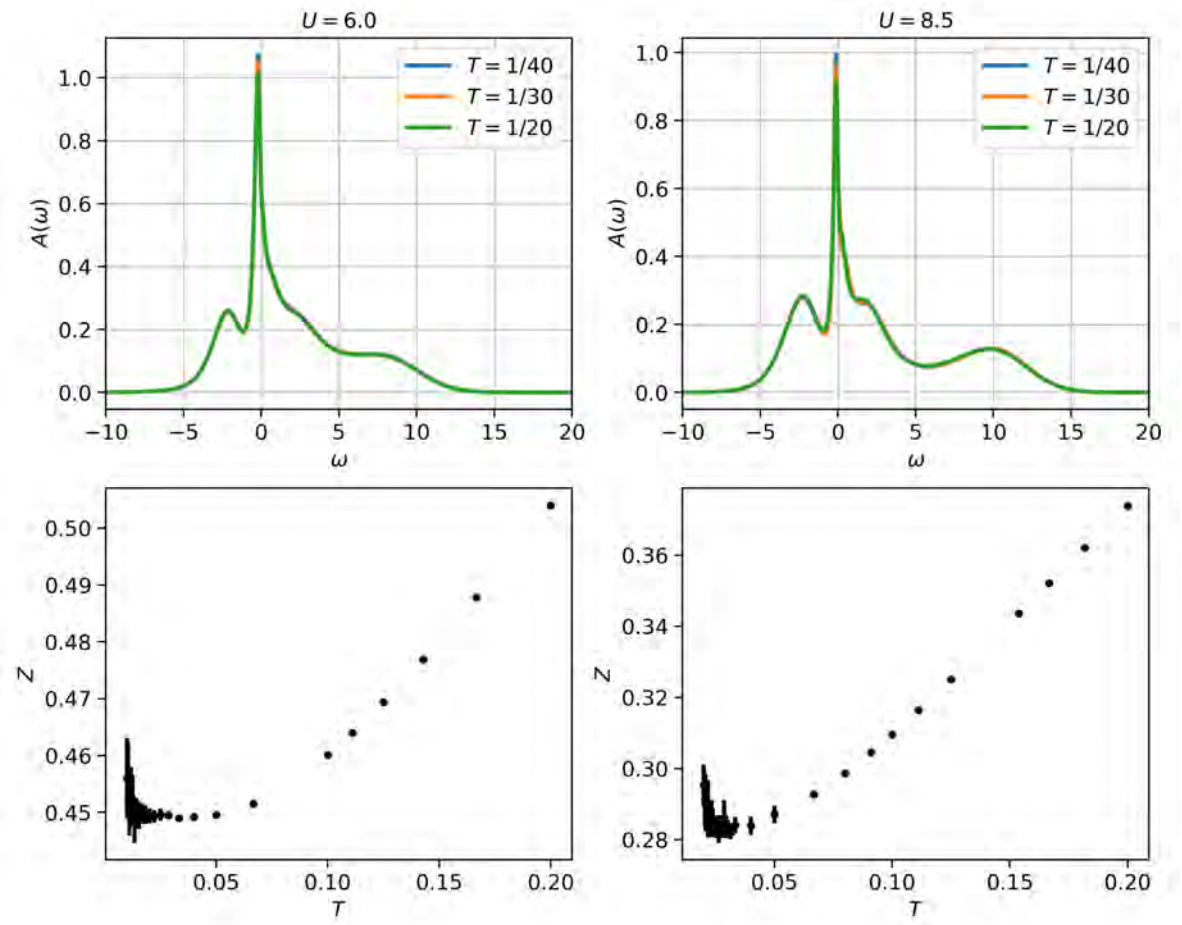

FIG. 7. Density of state for $p = 0.25$ at $T = 1/20$, $T = 1/30$ and $T = 1/41$ obtained from the maximum entropy method.

15. Fig. 8: U_{c3} is not defined in the current manuscript.

As U_{c3} had no importance in this research, we removed this line from the $U - -T$.

16. Typos:
(a) p. 1, left column: "on scattering" → "on the scattering", "value of" → "values of".
(b) p. 3, left column: "One of he" → "One of the". Right column: "higher the" → "higher than the".
(c) p. 5, right column: "near that T = 0.05" → "near T = 0.05".
(d) p. 8, left column, formatting error: A point "." went to a new line instead of remaining at the end of the respective sentence.
(e) p. 8, left column: "disorder on scattering" → "disorder on the scattering".

Thank you for the suggestions and for pointing out the above mistakes. The changes were made to

the manuscript.

[1] A. Szasz, J. Motruk, M. P. Zaletel, and J. E. Moore, Chiral Spin Liquid Phase of the Triangular Lattice Hubbard Model: A Density Matrix Renormalization Group Study, Phys. Rev. X **10**, 021042 (2020).

[2] A. Wietek, R. Rossi, F. Šimkovic, M. Klett, P. Hansmann, M. Ferrero, E. M. Stoudenmire, T. Schäfer, and A. Georges, Mott Insulating States with Competing Orders in the Triangular Lattice Hubbard Model, Phys. Rev. X **11**, 041013 (2021).

[3] H. Morita, S. Watanabe, and M. Imada, Nonmagnetic Insulating States near the Mott Transitions on Lattices with Geometrical Frustration and Implications for κ-$(ET)_2Cu_2(CN)_3$, Journal of the Physical Society of Japan **71**, 2109 (2002), https://doi.org/10.1143/JPSJ.71.2109.

[4] B. Kyung and A.-M. S. Tremblay, Mott transition, antiferromagnetism, and d-wave superconductivity in two-dimensional organic conductors, Physical Review Letters **97**, 046402 (2006).

[5] P. Sahebsara and D. Sénéchal, Hubbard Model on the Triangular Lattice: Spiral Order and Spin Liquid, Phys. Rev. Lett. **100**, 136402 (2008).

[6] M. Laubach, R. Thomale, C. Platt, W. Hanke, and G. Li, Phase diagram of the Hubbard model on the anisotropic triangular lattice, Physical Review B **91**, 245125 (2015).

[7] K. Misumi, T. Kaneko, and Y. Ohta, Mott transition and magnetism of the triangular-lattice hubbard model with next-nearest-neighbor hopping, Phys. Rev. B **95**, 075124 (2017).

[8] L. F. Tocchio, F. Becca, A. Parola, and S. Sorella, Role of backflow correlations for the nonmagnetic phase of the t–$t^{'}$ hubbard model, Phys. Rev. B **78**, 041101 (2008).

[9] T. Yoshioka, A. Koga, and N. Kawakami, Quantum phase transitions in the hubbard model on a triangular lattice, Phys. Rev. Lett. **103**, 036401 (2009).

[10] H.-Y. Yang, A. M. Läuchli, F. Mila, and K. P. Schmidt, Effective Spin Model for the Spin-Liquid Phase of the Hubbard Model on the Triangular Lattice, Phys. Rev. Lett. **105**, 267204 (2010).

[11] B.-B. Chen, Z. Chen, S.-S. Gong, D. N. Sheng, W. Li, and A. Weichselbaum, Quantum Spin Liquid with Emergent Chiral Order in the Triangular-Lattice Hubbard Model, Physical Review B **106**, 094420 (2022).